

Received April 9, 2017, accepted April 28, 2017, date of publication May 26, 2017, date of current version June 27, 2017.

Digital Object Identifier 10.1109/ACCESS.2017.2703614

On the Unambiguous Distance of Multicarrier Phase Ranging With Random Hopped Frequencies

PENG LIU¹, (Member, IEEE), WANGDONG QI¹, (Member, IEEE),
YUE ZHANG², AND LI WEI¹

¹P. L. A. University of Science and Technology, Nanjing 210007, China

²Beijing Satellite Navigation Center, Beijing 100094, China

Corresponding author: Wangdong Qi (wangdongqi@gmail.com)

This work is supported by the National Natural Science Foundation of China under Grant 61273047, Grant 61402520, Grant 61573376, Grant 61071115, Grant 61303267, and Grant 61601511.

ABSTRACT Multicarrier phase ranging (MCPR) technique has been widely used in radio navigation, telemetry, radar, and many other fields. In an MCPR system, unique range estimation can be obtained within only the so-called unambiguous distance (UD) because of phase ambiguity. As a metric gauging, the measurable distance of an MCPR system, the UD has been well studied under two common configurations: the linearly spaced frequencies and the proportionally spaced frequencies. In this paper, we propose to apply the frequency hopping (FH) waveform to the MCPR systems for an enhanced antijamming capability, which has been a key criterion in military and other mission critical applications. It is, however, difficult to define the UD with randomly spaced frequencies (RSF) led by the FH waveform. Under the RSF configuration, the UD becomes a random variable. We try to depict its statistical property with a deterministic value and find that the upper bound of the random UD plays an important role. We prove that, without phase noise, the UD can reach its upper bound with a large probability when only a dozen of carriers are employed, as long as the hop set of FH waveform is large enough. Simulations further show that even in the presence of phase noise and multipath fading scenarios the UD under the RSF configuration can also achieve its upper bound asymptotically if the number of carriers is moderately increased from a dozen to several dozens. Our paper uncovers the feasibility of applying the FH waveform to the MCPR systems.

INDEX TERMS Multi-carrier phase ranging, unambiguous distance, frequency hopping waveform.

I. INTRODUCTION

Carrier phase measurement can be used to estimate the distance that radio signal travels since the latter is proportional to the phase shift between the received and transmitted signal. This ranging technique has been widely used in many fields, such as radio navigation [1]–[3], telemetry [4], deep space ranging [5], radar [6], smart sensor and RFID tag localization [7], [8], optical interferometer [9], and wireless network security [10]. A well known problem with carrier phase ranging is phase ambiguity. When the distance to be measured is larger than the carrier wavelength, the number of whole cycles cannot be directly fixed by a single phase measurement. To resolve phase ambiguity, it is common to employ multiple carrier frequencies during one ranging cycle for joint estimation [1]–[9].

Even in a multi-carrier phase ranging (MCPR) system, phase ambiguity cannot be eliminated completely. Only if the distance is constrained within a specific interval called

as the unambiguous distance (UD), a unique estimation can be obtained. Therefore, the UD serves as a metric gauging the maximum measurable distance of an MCPR system. The size of UD depends on the set of carrier frequencies used for ambiguity resolution, i.e. $\{f_i\}$ ($i = 1, \dots, M$). Two common configurations of $\{f_i\}$ include linearly spaced frequencies (LSF) and proportionally spaced frequencies (PSF), as shown in Fig. 1(a) and 1(b) respectively. In the former case, the UD is the synthetic wavelength¹ of two adjacent carriers, i.e. $c/\Delta f$, where c is the signal propagation speed and Δf is the frequency step [3], [7]. In the latter case, the UD is just the largest carrier wavelength itself [4].

Recently, there has been a realistic need for enhancing the anti-jamming capability of radio positioning/navigation systems since they are becoming an important information

¹It is also called as the lane width in some radio navigation systems such as [1] and [3].

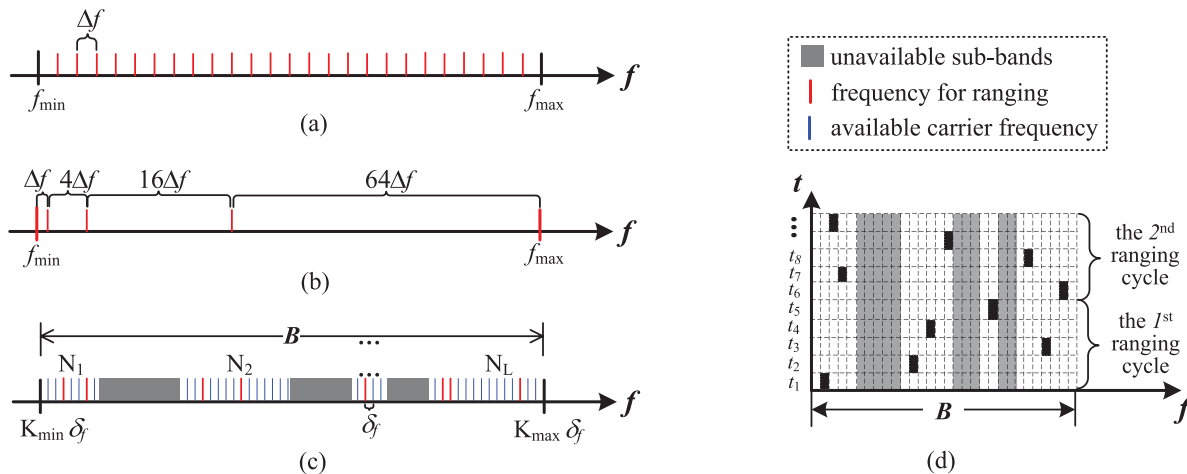


FIGURE 1. Configurations of the carrier frequencies in an MCPR system.

infrastructure [20], [21]. Frequency hopping (FH) waveform has been widely used in tactical and commercial radio communication networks for anti-jamming purposes [23]–[25]. In the FH waveform, the carrier frequency switches quickly amongst the hop set under the control of a random hopping sequence, as shown in Fig. 1(d). Since the hop set usually consists of a large number of channels and the hopping sequence is difficult to follow or predict, the FH waveform can evade jamming signals effectively. In this paper, we propose to apply the FH waveform to MCPR systems for an enhanced anti-jamming capability. However, the application of FH waveform also brings a new problem: *the carrier frequencies employed during one ranging cycle are randomly spaced within the bandwidth, as shown in the red lines of Fig. 1(c), and it is not clear how to define the UD in terms of randomly spaced frequencies (RSF)*. The challenge lies in that the corresponding UD, Λ_{rsf} , is a random variable and its statistical property is difficult to describe since the phase ambiguity resolution is a non-linear estimation problem.

In this paper, we aim to find a deterministic value instead of a random variable to depict the measurable distance of MCPR systems under the RSF configuration. It is safe to adopt the lower bound of the random UD as the metric, but it also drastically underestimates the practical performance. We then turn to explore the feasibility of using the upper bound, $\bar{\Lambda}_{rsf}$, as the metric.

We firstly derive the expression for $\bar{\Lambda}_{rsf}$ and prove that the necessary and sufficient condition for random UD achieving this upper bound is the carrier frequencies $\{f_i\}$ ($i = 1, \dots, M$) are relatively prime. By means of growth estimation technique in number theory, we further derive an elegant closed-form expression to approximately describe the probability of $\{f_i\}$ being relatively prime, i.e. P_M . We are inspired to find that, as long as the hop set of FH waveform consists of a large number of channels, P_M will approach 1 when only a dozen of carrier frequencies are employed. This conclusion is well supported by numerical simulations. As to a

fast frequency hopping waveform, 1000 hops per second for example, the corresponding ranging cycle takes just a dozen of milliseconds.

The above analysis is based on the assumption that phase error is absent. We further investigate the impact of phase error on the UD under the RSF configuration through extensive simulations. It has been reported that the size of UD under the LSF configuration varies significantly depending on whether phase error is neglectable or not [9]. One may anticipate a similar result for the RSF configuration. Fortunately, the simulation results show that, even in the presence of random noise and multipath induced phase error, the UD under the RSF configuration can still achieve its upper bound $\bar{\Lambda}_{rsf}$ asymptotically as long as the number of carriers M are moderately increased from a dozen to several dozens. As a comparison, to obtain the same theoretical UD under the LSF and PSF configurations, an order more carriers or extremely accurate phase measurement would be a necessary condition.

The contributions of this paper are summarized as follows:

- The FH waveform is firstly introduced into MCPR systems for an enhanced anti-jamming capability.
- We prove that, when phase error is absent, the upper bound of the random UD $\bar{\Lambda}_{rsf}$ can serve as a trustworthy metric of the measurable distance for MCPR systems employing the FH waveform, as long as the frequency hop set is large enough.
- Simulations further show that $\bar{\Lambda}_{rsf}$ can also be achieved probably even in the presence of phase noise and multipath induced phase error.

The remainder of the paper is organized as follows. In Section II, we provide a brief review about the related works. In Section III, we present the system model for an MCPR system employing the FH waveform. The analysis on the UD of the RSF configuration in the absence of phase error is provided in Section IV, followed by the numerical simulations. In Section V, we study the impact of phase error on the UD under the RSF configuration through

extensive simulations. Finally, conclusions are achieved in Section VI.

II. RELATED WORKS

The unambiguous distance of an MCPR system defines its measurable distance, and it has received many research interests [1], [3], [6], [7], [9]. The size of UD depends on the carrier frequencies used for phase ambiguity resolution. If only a single carrier is used, the UD is obviously the wavelength itself. An MCPR system under the PSF configuration is just the case. In such a system, phase ambiguity is resolved in a cascading manner, i.e., the range estimation obtained from the carrier with a longer wavelength is used to resolve the phase ambiguity of the carrier with a shorter wavelength. Therefore, the UD of the system is limited by the longest wavelength. In telemetry applications, the synthetic carrier wavelength may be as long as tens of thousands of kilometers to guarantee a large measurable distance [4].

Under the configuration of dual carrier frequencies² $\{f_1, f_2\}$, a widely accepted metric of UD is the synthetic wavelength of these two frequencies, i.e. $\Lambda = c/\Delta f$, where $\Delta f = |f_1 - f_2|$ [3]. Take the carrier phase GPS for example. When the frequencies of $L1$ (1575.42MHz) and $L2$ (1227.60MHz) are employed, the synthetic wavelength is $c/(L1 - L2) = 86.2\text{cm}$, nearly 4 times larger than the original wavelength. Actually, the theoretical UD, which is the least common multiple of the two carrier wavelengths [14], is much larger than the synthetic wavelength. In the above example, the theoretical value of UD with frequencies $L1$ and $L2$ is 14.66m , 17 times larger than the synthetic wavelength. However, the theoretical UD with dual carriers can only be obtained when the phase error is small enough [9]. Otherwise, the synthetic wavelength is still a good metric for gauging the measurable distance of an MCPR system.

The UD with more than two carrier frequencies has been investigated in [2], [6], and [7]. Under the LSF configuration, UD can still be depicted by the synthetic wavelength, i.e., $c/\Delta f$. A smaller frequency step results in a larger UD. However, the bandwidth also shrinks which leads to a deteriorated ranging accuracy [6]. Alternatively, more carriers can be used to occupy a large bandwidth. For example, a radio navigation system in [2] employs 192 frequencies to enlarge the UD to kilometer level, but one measurement cycle takes as long as 6 seconds, leading to a poor real time performance.

In [11], a mechanism has been designed to select carrier frequencies randomly for an MCPR system. It is observed that the UD can be significantly enlarged compared with the LSF configuration, but no solid explanation is provided. Furthermore, the mechanism proposed in [11] adopts two independent randomization process, which does not agree with the model of FH waveform as shown in Fig. 1(d).

Finally, it is worthy to note that, although the FH waveform has already been applied to an MCPR radar system [6], the UD of such an FH radar is still a deterministic value.

The reason lies in that all the frequencies in the hop set are used for ambiguity resolution. Essentially, this configuration degenerates to an LSF case. In this paper, we are concerned to describe the random UD when only a random subset of the hop set is used for ambiguity resolution.

III. SYSTEM MODEL

In this section, we provide the model for an MCPR system, including the configuration of carrier frequencies as well as the phase ambiguity resolution.

A. CONFIGURATION OF CARRIER FREQUENCIES

Under the LSF configuration, as shown in Fig. 1(a), the set of carrier frequencies $\{f_i\}$ is an arithmetic sequence, i.e., $f_{i+1} = f_i + \Delta f$ ($i = 1, \dots, M - 1$). Given the bandwidth \mathbf{B} , the number of carrier frequencies can be represented as $M = \mathbf{B}/\Delta f$. On one hand, a smaller frequency step leads to a larger UD because $\Lambda_{lsf} = c/\Delta f$ [7]. On the other hand, a larger bandwidth \mathbf{B} results in a better ranging accuracy [6], [13]. Therefore, M would be increased to achieve good performance at both ends. In practical MCPR system that employs the LSF configuration, M varies from 2 to several hundreds. A larger M means a longer measurement cycle, and thus poorer real time performance.

Under the PSF configuration, as shown in Fig. 1(b), the frequency step of $\{f_i\}$ is a geometric sequence, i.e. $\Delta f_{i+1} = \mu \Delta f_i$ ($i = 1, \dots, M - 1$) where μ is a positive integer. The UD under the PSF configuration is determined by the longest synthetic wavelength, i.e. $\Lambda_{psf} = c/\Delta f_1$. Since Δf_i enlarges exponentially, the number of carriers M is much smaller than that under the LSF configuration given the same bandwidth \mathbf{B} . In telemetry applications that employs the PSF configuration, M is usually no more than 10.

The application of the FH waveform to an MCPR system results in the random spaced frequencies (RSF) configuration, as shown in the red lines of Fig. 1(c). In the FH waveform, the carrier frequency switches quickly amongst the hop set $\Phi = \{f_i\}$ ($i = 1, \dots, N$) under the control of a random hopping sequence, as shown in Fig. 1(d). In general, Φ itself is just a LSF set and N is large enough, as shown in the blue lines of Fig. 1(c). The elements of the hopping sequence are integers k_i ($i = 1, \dots, N$) which map to the carrier frequencies f_i with the equation $f_i = k_i \delta_f$ where δ_f is the frequency step of the hop set. During one ranging cycle, the phase of M ($M \ll N$) carriers are measured for ambiguity resolution.³ To evade jamming signals effectively, the hopping sequence should be as random and uniform as possible [26]. Therefore, it is equivalent to randomly choose M frequencies from the hop set Φ following the uniform distribution. The non-continuity of the bandwidth \mathbf{B} under the RSF configuration is taken into consideration for two reasons: (i) in the dynamic spectrum access paradigm enabled by cognitive radios, the distribution of available spectrum is

³If $M = N$, the RSF configuration degenerates to the LSF configuration and the measurement time for one ranging cycle enlarges correspondingly.

²It is regarded as a special case of the LSF configuration in this paper.

TABLE 1. Symbols for describing different configurations of carrier frequencies.

Symbol	Definition	Comment
Λ	The UD of an MCPR system	
Φ	The frequency hop set of the FH waveform	
δ_f	The frequency step of Φ	
\mathbf{B}	The bandwidth of Φ under the RSF configuration	
N	The number of carriers in Φ	A large integer
f_i	The i -th carrier frequency in Φ	$i = 1, \dots, N$
k_i	The value of frequency register corresponding to f_i	$k_i = f_i/\delta_f$
\mathbb{K}	The set of integers $\{k_i\}$	
\mathbb{F}	The set of carrier frequencies used within one ranging cycle for ambiguity resolution	A random subset of Φ
M	The number of carriers in \mathbb{F}	$M \ll N$
Δf	The frequency step of \mathbb{F}	δ_f or a multiple of δ_f
L	The number of segments \mathbf{B} is divided into	A small integer
N_l	The number of frequencies that the l -th segment consists of	
μ	The scale factor of the frequency step under the PSF configuration	A positive integer

often non-contiguous [12]; (ii) the FH waveform can readily aggregate the non-contiguous bandwidth to further improve the anti-jamming capability as well as the ranging accuracy of an MCPR system [13].

We denote \mathbb{K} as the set of positive integers $\{k_i\} (i = 1, \dots, N)$. The minimum and maximum value of $\{k_i\}$ is K_{min} and K_{max} respectively. Due to the non-continuity of the bandwidth \mathbf{B} , the integers in \mathbb{K} is also non-contiguous. We divide \mathbb{K} into L sub-sets, each containing N_l contiguous integers. So the norm of \mathbb{K} can be represented as $N = \sum_{l=1}^L N_l$.

The symbols used to describe the LSF, PSF and RSF configurations are summarized in Table 1.

B. AMBIGUITY RESOLUTION OF AN MCPR SYSTEM

In an MCPR system, phase shift between the reference and received signals are measured at multiple carrier frequencies for ambiguity resolution. Denoting the reference signals as $x(t) = A_t \cos(2\pi f_i t) \{i = 1, \dots, M\}$, then the received signal is the addition of the delayed signal and channel noise, i.e., $y(t) = B_t \cos(2\pi f_i (t - d/c)) + w(t)$, where A_t and B_t are signal amplitudes, d is the distance that radio signal travels, c is the signal propagation speed, and $w(t)$ is the channel noise.

The theoretical values of phase shifts between the reference and received signals are

$$\varphi_i^0 = 2\pi f_i \frac{d}{c} \pmod{2\pi}. \tag{1}$$

Due to the modulo operation, there exists ambiguity when deducing d from the phase measurements. Eqs. (1) can also be written as

$$d = n_i \lambda_i + \frac{\varphi_i^0}{2\pi} \lambda_i, \tag{2}$$

where $\lambda_i = c/f_i$ is the wavelength of the i -th carrier, n_i is the whole cycle ambiguity. Under the PSF configuration, n_i is solved iteratively by n_{i-1} while n_1 is determined by *a-priori* knowledge about d . Under the LSF and RSF configurations, d and n_i are solved together by phase measurements. However, Eqs. (2) are underdetermined, and therefore, the solution of d is not unique. These solutions are spaced apart with the cycle of the least common multiple of λ_i [14], which is referred as the UD. A unique solution of d can only be obtained if d is constrained within the UD.

In the presence of phase error, analytical solution to Eqs. (2) is not available. Alternatively, ambiguity can be resolved by some estimation techniques, such as phase unwrapping [19] and least square estimation [7]. Denoting the phase measurement as $\varphi_i = \varphi_i^0 + n_i$ where n_i is the phase error. In this paper, we adopt the least square estimator

$$\tilde{d} = \arg_d \min F(d) \quad s.t. \quad d \in \mathbf{D}, \tag{3}$$

where $F(d) = \sqrt{\sum (\varphi_i - 2\pi \langle \frac{d}{\lambda_i} \rangle)^2}$ is the square error of the estimation d , $\langle x \rangle$ is the fractional part of x , and \mathbf{D} is the search interval. In the presence of phase error, there exist two kinds of ranging error, i.e. local small error and outliers [13]. Since the uniqueness of distance estimation is not feasible, we have to make a new definition of the practical UD with phase error.

Definition 1: The practical UD of MCPR systems after phase errors have been introduced is the maximum search interval \mathbf{D} which satisfies that $Pr(|\tilde{d} - d_0| \leq \ell) > P_{thre}$, where d_0 is the true distance while \tilde{d} is the estimated distance based on the objective function (3), ℓ is the threshold for non-outlier estimation, P_{thre} is the threshold for the probability of non-outliers, $|x|$ and $Pr(x)$ denotes the absolute value and the probability of x respectively.

In other words, the practical UD is the maximum search interval to guarantee the probability of non-outlier estimations is large enough, say 99.9%. In Section V, we will analyze the impact of phase error on the practical UD quantitatively.

IV. UNAMBIGUOUS DISTANCE UNDER THE RSF CONFIGURATION WITHOUT PHASE ERROR

In this section, we firstly derive the lower and upper bound of theoretical UD under the RSF configuration, and then analyze the probability of UD achieving its upper bound $\bar{\Lambda}_{rsf}$ in the absence of phase error. Finally, numerical simulation results are provided to verify the theoretical analysis.

A. THE LOWER AND UPPER BOUND OF UD

As stated in Section III, without phase error, the theoretical UD is the least common multiple of the carrier wavelengths used for ambiguity resolution. Theorem 1 describes the theoretical UD in terms of the carrier frequencies $\{f_i\} (i = 1, \dots, M)$.

Theorem 1: The theoretical UD of an MCPR system can be expressed as follows:

$$\Lambda = \frac{c}{\kappa \delta_f}, \quad (4)$$

where κ is the greatest common divisor of $\{k_i\}$ ($i = 1, \dots, M$).

Proof: Since $\Lambda = a_i \cdot \lambda_i$ (a_i is an integer) and $\lambda_i = \frac{c}{k_i \delta_f}$, we turn to find the least common multiple of $\{1/k_i\}$. Denoting $1/\kappa'$ as one of the common multiples of $\{1/k_i\}$. Since $1/\kappa'$ is divisible by $1/k_i$ if and only if k_i is divisible by κ' , it is obvious that κ' is the common divisor of $\{k_i\}$. If κ' is the greatest common divisor of $\{k_i\}$, i.e. κ , then its inverse is the least common multiple of $\{1/k_i\}$. Therefore, Λ could be expressed as $\frac{c}{\kappa \delta_f}$. \square

Based on Theorem 1, we can easily conclude the lower and upper bounds of the UD under the RSF configuration. On one hand, the greatest common divisor of $\{k_i\}$ is no greater than K_{min} , thus the lower bound can be represented as

$$\tilde{\Lambda}_{rsf} = \frac{c}{K_{min} \delta_f} = \lambda_{max}. \quad (5)$$

This lower bound is achieved only under the extreme condition that all the frequencies in the RSF configuration are a multiple of $(K_{min})\delta_f$. For modern radio positioning/navigation systems employing the UHF or L band, the maximum carrier wavelength is on the meter level or below. It is safe but over-conservative to adopt such a value as the metric for the measurable distance under the RSF configuration.

On the other hand, the upper bound can be represented as

$$\bar{\Lambda}_{rsf} = \frac{c}{\delta_f}. \quad (6)$$

Furthermore, we obtain the following lemma without additional proof.

Lemma 1: $\bar{\Lambda}_{rsf}$ can be obtained if and only if the integers in $\{k_i\}$ ($i = 1, \dots, M$) are relative prime.

Remark: According to Eq. (6), a smaller δ_f results in a larger $\bar{\Lambda}_{rsf}$. The frequency step adopted by the FH waveform is usually on the order of KHz [27]. Correspondingly, the upper bound of the random UD may be up to tens of or even hundreds of kilometers, large enough for most radio positioning/navigation applications. So the key problem left is how probable that the M -tuple $\{k_i\}$ being relative prime and how this probability varies with respect to the number of carriers M .

B. THE PROBABILITY OF OBTAINING $\bar{\Lambda}_{rsf}$

As revealed by Lemma 1, the probability that UD under RSF configuration obtains its upper bound is equivalent to the probability that M random algebraic integers $\{k_i\}$ being relative prime. In the field of analytical number theory, a similar problem has been solved by the Benkoski's theorem [16]. However, these random integers are required to be chosen from a continuous set $[1, N]$. Here, we try to tackle the

difficulties arising from the non-continuous candidate set \mathbb{K} ($L \geq 1$) and arbitrary starting point K_{min} under the RSF configuration.

Denoting the probability that integers $\{k_i\}$ ($i = 1, \dots, M$) randomly chosen from \mathbb{K} are relative prime as P_M . The value of P_M is depends not only on M , but also on the number of sub-bands, L , as well as the distribution of these sub-bands. Under the assumption that L and M are the constants much smaller than N , we manage to specify the "growth" of P_M with respect to these parameters using the growth estimation tool borrowed from the analytic number theory.

Theorem 2: The probability that M random integers $\{k_i\}$ out of \mathbb{K} being relative prime can be approximated as

$$P_M \approx \frac{1}{\zeta(M)},$$

where $\zeta(\cdot)$ is the Riemann-zeta function.

Proof: Firstly, we define the following notations.

- p_1, \dots, p_N : a serial of distinct primes;
- A_{p_1, \dots, p_N} : the number of M -tuples composed with positive integers in \mathbb{K} which can be divided by $\prod_{i=1}^N p_i$;
- Z : the number of relative prime M -tuples composed with integers out of \mathbb{K} .

Obviously, $P_M = Z/N^M$. So we concentrate on deriving the expression for Z .

These integers in the M -tuple are relative prime if and only if there exists no prime that divides all M integers. According to the Inclusion-Exclusion principle, we have

$$Z = N^M - \sum_{p_1} A_{p_1} + \sum_{p_1 < p_2} A_{p_1 p_2} - \sum_{p_1 < p_2 < p_3} A_{p_1 p_2 p_3} + \dots \quad (7)$$

Let x_j represents the number of integers in \mathbb{K} that can be divided by the integer j , then x_j^M is the number of M -tuples that can be divided by the integer j , and we have $\sum_{p_1} A_{p_1} = x_2^M + x_3^M + x_5^M + x_7^M + \dots$, $\sum_{p_1 < p_2} A_{p_1 p_2} = x_{2*3}^M + x_{2*5}^M + x_{2*7}^M + \dots$, and so on. By using the Möbius function μ , Eq. (7) can be reformatted more compactly as

$$Z = \sum_{j=1}^{\infty} \mu(j) x_j^M, \quad (8)$$

where $\mu(j)$ is the Möbius function defined as

$$\mu(j) = \begin{cases} 1 & \text{if } j = 1; \\ 0 & \text{if } j \text{ has repeated prime factors;} \\ (-1)^r & \text{if } j \text{ has } r \text{ different prime factors.} \end{cases}$$

Actually, we do not need the infinity at the upper end of the summation in Eq. (8), since the terms with $j > K_{max}$ are all zeros. So we further rewrite the sum as

$$Z = \sum_{j=1}^{K_{max}} \mu(j) x_j^M. \quad (9)$$

Let N_l and $x_j(l)$ denote the number of integers in the l -th segment of \mathbb{K} and those can be divided by j respectively, then

$N = \sum_{l=1}^L N_l$, $x_j = \sum_{l=1}^L x_j(l)$. Since each pair of adjacent integers that can be divided by j are spaced apart with j , the maximum of $x_j(l)$ is $\lceil N_l/j \rceil$ while its minimum is $\lfloor N_l/j \rfloor$. So we have $\sum_{l=1}^L (N_l/j - 1) < x_j(l) < \sum_{l=1}^L (N_l/j + 1)$, that is, $N/j - L < x_j < N/j + L$. Furthermore, under the assumption that L is a small constant independent of N , we have $x_j = \mathbf{O}(\frac{N}{j})$.

Since

$$x_j^M - \left(\frac{N}{j}\right)^M = \left(x_j - \frac{N}{j}\right) \left(x_j^{M-1} + x_j^{M-2} \left(\frac{N}{j}\right) + \dots + \left(\frac{N}{j}\right)^{M-1}\right),$$

and $0 \leq N/j - x_j \leq L$, we have

$$x_j^M - \left(\frac{N}{j}\right)^M = \mathbf{O}\left(\left(\frac{N}{j}\right)^{M-1}\right). \tag{10}$$

Applying the growth estimate of Eq. (10) to Eq. (9), we have

$$Z = \sum_{j=1}^{K_{max}} \mu(j) \left(\frac{N}{j}\right)^M + \mathbf{O}\left(\sum_{j=1}^{K_{max}} \left(\frac{N}{j}\right)^{M-1}\right). \tag{11}$$

Therefore, P_M can be represented as

$$P_M = \frac{Z}{N^M} = \sum_{j=1}^{K_{max}} \left(\frac{\mu(j)}{j^M}\right) + \mathbf{O}\left(N^{-1} \sum_{j=1}^{K_{max}} \left(\frac{1}{j^{M-1}}\right)\right). \tag{12}$$

As proved in [17], the summation of Dirichlet series $\frac{\mu(j)}{j^M}$ is

$$\sum_{j=1}^{\infty} \frac{\mu(j)}{j^M} = \frac{1}{\zeta(M)}.$$

So, the first sum in Eq. (12) can be rewritten as

$$\begin{aligned} \sum_{j=1}^{K_{max}} \frac{\mu(j)}{j^M} &= \frac{1}{\zeta(M)} - \sum_{j=K_{max}+1}^{\infty} \frac{\mu(j)}{j^M} \\ &= \frac{1}{\zeta(M)} + \mathbf{O}\left(\int_{K_{max}+1}^{\infty} \frac{dx}{x^M}\right) \\ &= \frac{1}{\zeta(M)} + \mathbf{O}\left((K_{max} + 1)^{1-M}\right). \end{aligned} \tag{13}$$

To simplify the analysis, we assume $M \geq 3$. When $N \rightarrow \infty$, K_{max} also approaches to the infinity. Since $M \geq 3$, we have $\mathbf{O}((K_{max} + 1)^{1-M}) \rightarrow 0$.

For the second term in Eq. (12), also under the condition that $M \geq 3$ and $K_{max} \rightarrow \infty$, we have

$$\sum_{j=1}^{K_{max}} \frac{1}{j^{M-1}} = \mathbf{O}\left(\int_1^{K_{max}} \frac{dx}{x^{M-1}}\right) = \mathbf{O}(1),$$

and thus, this term is on the order of $\mathbf{O}(N^{-1})$, which also approaches to 0 when $N \rightarrow \infty$.

Finally, we conclude that

$$\lim_{N \rightarrow \infty} P_M = \frac{1}{\zeta(M)}. \tag{14}$$

The number of available frequencies of the FH waveform, N , is usually on the order of tens of thousands in engineering systems. In such a condition, the approximation made in Theorem 2 is good enough to specify the probability of the M -tuple $\{k_i\}$ randomly chosen from \mathbb{K} being relative prime. \square

Remark: When $M > 1$, the Riemann-zeta function is always a positive number larger than 1, and it converges to 1 rapidly as M increases. Therefore, the approximated probability of $\{k_i\}$ ($i = 1, \dots, M$) being relative prime approaches to 1 as M increases. Since the upper bound of the random UD can be obtained with large probability, we propose to adopt this value as the metric of the measurable distance for an MCPR system under the RSF configuration.

C. NUMERICAL SIMULATION

As stated in Theorem 2, the probability of an M -tuple randomly chosen from \mathbb{K} being relative prime can be approximated with the inverse of Riemann-zeta function. In this section, we conduct numerical simulations using the Monte-Carlo method to examine the accuracy of this approximation. In simulations, the bandwidth \mathbf{B} ranges from 132MHz to 862MHz, which is readily available for radio communication systems employing the FH waveform [23], [24]. The frequency resolution is $\delta_f = 1$ kHz. The hop set consists of $N = 2^{15}$ carrier frequencies which are distributed uniformly within \mathbf{B} . We examine three different scenarios where the number of spectrum segments L is 1, 7, and 12 respectively. M ranges from 3 to 13. The corresponding $\{k_i\}$ are chosen randomly from \mathbb{K} using an M -sequence generator. For each combination of M and L , 10^5 Monte-Carlo simulations are conducted, and then the probability of $\{k_i\}$ being relative prime is calculated.

Both the theoretical and simulation results on the probability P_M are given in Fig. 2. As shown in the figure, when the frequency hop set is large enough, the simulation results of P_M agree with the theoretical value in all scenarios. Therefore, the approximation made in Theorem 2 is accurate enough. Another important observation is that P_M approaches 1 very closely when $M > 10$ no matter how many segments the bandwidth is composed with. A small M means a short ranging cycle while a large N leads to a large UD. Therefore, the size of UD under the RSF configuration can be easily extended without sacrificing the real time performance.

V. THE IMPACT OF PHASE ERROR ON THE PRACTICAL UNAMBIGUOUS DISTANCE

In this section, we study the impact of phase error on the practical UD of the RSF configuration through extensive simulations. Particularly, we investigate two different kinds of phase error, i.e. random noise and multipath induced error.

As defined in Section III, a practical UD is the maximum interval within which the probability of non-outliers is large

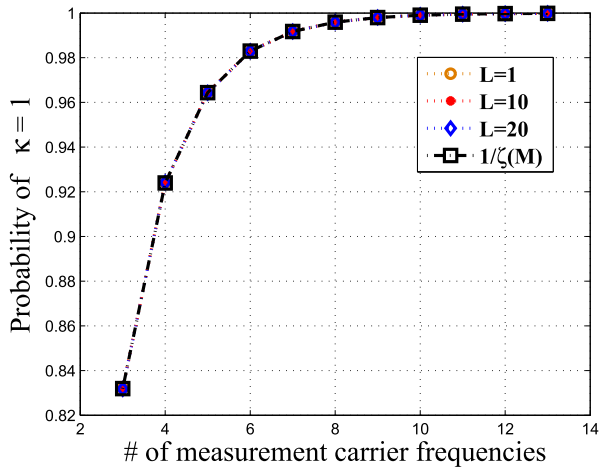


FIGURE 2. Probability of M -tuple $\{k_i\}$ out of \mathbb{K} being relative prime.

enough. Under the RSF configuration, a distance estimation \tilde{d} is regarded as a non-outlier if $|\tilde{d} - d_0| < c/(\Delta f)_{max}$, where $(\Delta f)_{max}$ is the maximum step of any two adjacent frequencies in the RSF configuration.⁴ We try to find out whether the practical UD under the RSF configuration can achieve $\bar{\Lambda}_{rsf}$.

A. PRACTICAL UD WITH RANDOM PHASE NOISE

Phase noise is modeled as an i.i.d random variable following the zero mean Gaussian distribution. We consider two cases with the standard deviation of $\sigma = 0.1$ rad and $\sigma = 0.5$ rad, respectively. The lowest carrier frequency is 131.9 MHz and the frequency step of the hop set is $\delta_f = 1$ MHz. Correspondingly, the upper bound of the random UD is $\bar{\Lambda}_{rsf} = 300$ m. Choosing a large δ_f is to facilitate the analysis of the least square objective function. The true distance is 201m and the search interval for the least square estimator is $[51m, 351m]$. This search interval centers around the true distance and its length equals to $\bar{\Lambda}_{rsf}$. The number of carriers M varies from 3 to 200. For each M , we conduct 10^5 Monte-Carlo simulations and calculate the probabilities of non-outlier estimations. Simulation results under the RSF configuration are shown as the red lines in Fig. 3.

When the standard deviation of phase noise is small ($\sigma = 0.1$), the probability of non-outlier estimations within the interval of $\bar{\Lambda}_{rsf}$ converges to 1 when $M > 10$. This result agrees well with the Theorem 2. As the standard deviation of phase noise grows ($\sigma = 0.5$), the probability of non-outlier estimations drops moderately. But $\bar{\Lambda}_{rsf}$ can also be obtained asymptotically when $M > 20$.

1) COMPARISON WITH THE LSF CONFIGURATION

As a comparison, we construct a LSF configuration which also meets the criterion that carrier frequencies are relatively prime while the frequency step is $\Delta f = 6\delta_f$. Theoretically,

⁴A non-outlier is NOT an accurate estimation. Since the accuracy metric of an MCPR system is out of the scope of this paper, interested readers can refer to [13] for more information.

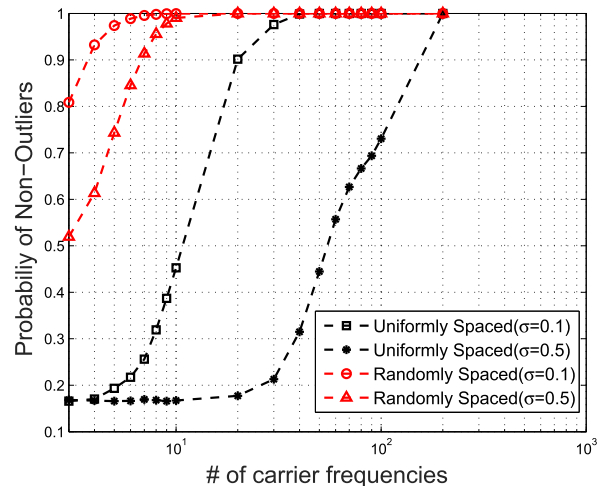


FIGURE 3. Probability of non-outlier estimation in the presence of Gaussian phase noise under the LSF and RSF configurations.

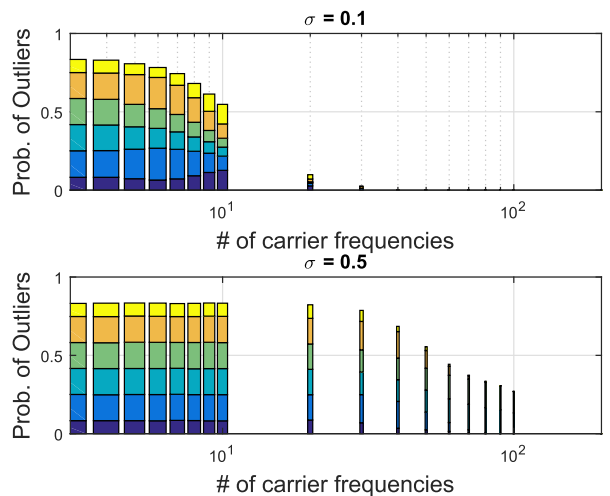


FIGURE 4. Probability of outliers under the LSF configuration after phase noise is introduced.

the UD under this LSF configuration is the same as that under the RSF configuration. We also conduct 10^5 Monte-Carlo simulations to investigate the impact of phase noise on the UD under the LSF configuration. An estimation \tilde{d} is regarded as a non-outlier if $|\tilde{d} - d_0| < c/(\Delta f)$. For each M , we choose the same bandwidth \mathbf{B} for the two configurations for fairness because \mathbf{B} also determines the ranging accuracy of an MCPR system [13]. The simulation results under the LSF configuration are shown as black lines in Fig. 3. Compared with the RSF configuration, the probability of non-outlier estimations under the LSF configuration drops dramatically when the number of carriers is decreased. The theoretical UD cannot be obtained asymptotically until M grows to several tens or hundreds.

To get some insight into this phenomenon, we further investigate the objective function of the least square estimator under the LSF and RSF configuration. Since the frequencies

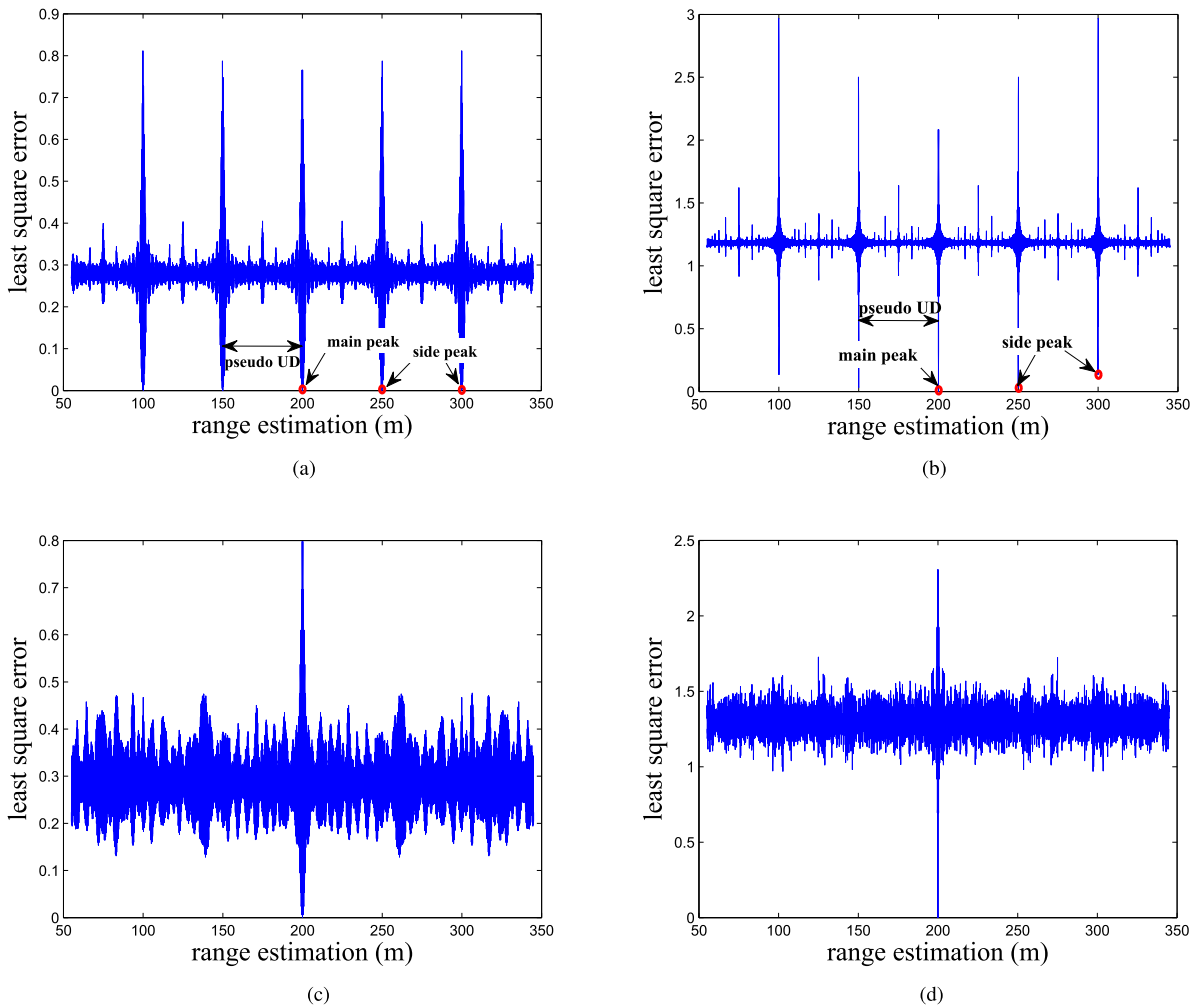


FIGURE 5. Objective function of the least square estimator under the LSF and RSF configurations. (a) $M=20$, LSF configuration. (b) $M=200$, LSF configuration. (c) $M=20$, RSF configuration. (d) $M=200$, RSF configuration.

under the LSF configuration are also relatively prime, the theoretical UD is also $\Lambda_{lsf} = 300$ m. However, the objective function under the LSF configuration has one main-lobe at the true distance and multiple side-lobes at the outliers within the interval of $\bar{\Lambda}_{lsf}$, as shown in Fig. 5(a) and 5(b). Even in the absence of phase noise, the peaks of these side-lobes are very close to that of the main-lobe. For example, the difference between the main peak ($d=201$ m) and these side peaks in Fig. 5(a) is less than 0.001. It is very difficult to distinguish the main peak from these side peaks after phase noise is introduced. Therefore, outliers will occur at these side peaks with large probability. The main peak is not distinguishable until M becomes larger, as shown in Fig. 5(b).

The probability of outliers under the LSF configuration after phase noise has been introduced is presented in Fig. 4. In line with the expectation, if M is small while the standard deviation of phase noise is large, the probability of each outlier is nearly equivalent to that of non-outlier estimation. These outliers are spaced apart with the cycle of 50 m, which

is just the synthetic wavelength $c/\Delta f$. Only if hundreds of carrier frequencies are employed under the LSF configuration, the probabilities of outliers is neglectable. Therefore, for an MCPR system which uses less than ten carrier frequencies, such as Omega and carrier phase GPS, it is the synthetic wavelength rather than the theoretical UD that is more suitable for gauging the measurable distance.

On the contrary, under the RSF configuration, although there also exist some side peaks in the objective function, they are distinguishable from the main peaks even M is small, as shown in Fig. 5(c). This is particularly true as M enlarges, indicated by Fig. 5(d). Correspondingly, the probability of outliers is small after phase noise has been introduced and it is feasible to adopt Λ_{rsf} as the UD under the RSF configuration.

2) COMPARISON WITH THE PSF CONFIGURATION

Finally, we compare the impact of phase noise on the practical UD under the RSF configuration against that under

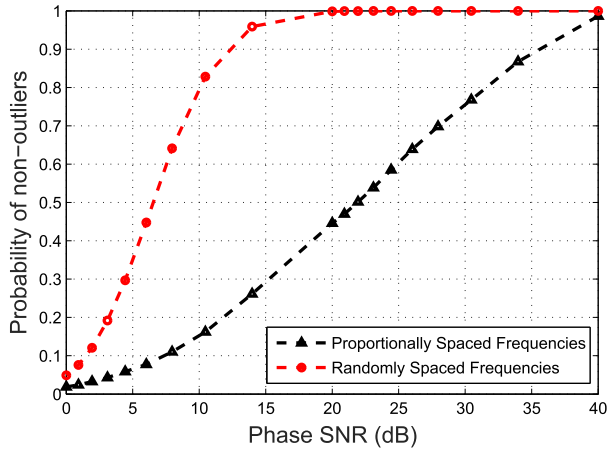


FIGURE 6. Probability of non-outliers in the presence of Gaussian phase noise under the LSF and PSF configurations.

the PSF configuration. Since the frequency step under the PSF configuration grows exponentially as the number of carriers M is increased, it is infeasible to employ a large M . We set $\Delta f_1 = 1\text{MHz}$ and $M = 7$. The theoretical UD is $\Lambda_{psf} = 300\text{m}$ which is set as the search interval. The largest frequency step is $\Delta f_6 = 1024\text{MHz}$ and the bandwidth is $\mathbf{B} = 1365\text{MHz}$. For the RSF configuration, \mathbf{B} and M are set the same as that of the PSF configuration. The standard deviation of Gaussian phase noise σ varies between 0.01 rad and 1 rad and 10^5 Monte-Carlo simulations are conducted for each σ . We define $10 \log \frac{1}{\sigma^2}$ as the signal-to-noise-ratio (SNR) of phase measurement and investigate the relationship between the probability of non-outliers and phase SNR. The simulation results under these two configurations are shown in Fig. 6.

Since M is small, the theoretical UD under the RSF configuration can only be obtained asymptotically when phase SNR is larger than 15dB. However, the asymptotical condition for obtaining the theoretical UD under the PSF configuration is even much stricter, since the probability of non-outliers approaches 1 only when phase SNR is larger than 40dB. If the phase SNR is not that high, it is convenient to increase the probability of non-outliers by employing more carriers under the RSF configuration while this method does not work under the PSF configuration.

B. PRACTICAL UD WITH MULTIPATH INDUCED PHASE ERROR

In this section, we turn to study the impact of multipath induced phase error on the practical UD. The multipath induced phase error is sensitive to channel parameters, and therefore, it is vulnerable to environment change and difficult to predict [22]. We model the phase error induced by multipath fading as i.i.d random variables following the zero-mean uniform distribution. This model has been verified by some in-site measurements [22]. For simplicity, Gaussian phase noise is ignored after multipath error has been introduced.

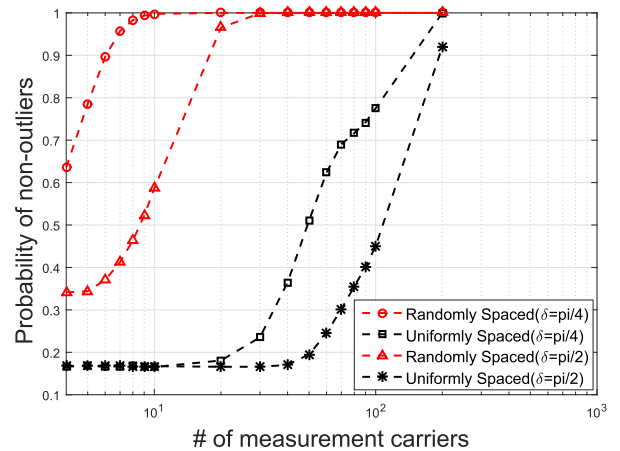


FIGURE 7. Probability of non-outliers in the presence of multipath induced phase error.

The parameter settings for Monte-Carlo simulations are the same with those in the previous section except for the phase error model. The multipath induced phase error is assumed to be uniformly distributed within $[-\delta, \delta]$. We consider a weak multipath environment where $\delta = \pi/4$ and a strong multipath environment where $\delta = \pi/2$ respectively. The probability of non-outliers under the RSF configuration is shown in Fig. 7 and it is only compared with that under the LSF configuration. Similar with Fig. 3, the practical UD under the RSF configuration is more robust against multipath error than that under the LSF configuration. Even in strong multipath environment, the probability of unambiguous estimation under the RSF configuration can approach 1 by employing only 20 carriers, whereas the minimum number of carriers needed by the LSF configuration to obtain the UD reliably is more than 200, an order more than that needed by the RSF configuration. More importantly, this result confirms that $\bar{\Lambda}_{rsf}$ can also serve as a practical metrics for the measurable distance of an MCPR system in multipath scenarios.

VI. CONCLUSION

This paper introduces the frequency hopping radio waveform into MCPR systems and explores the performance with respect of the unambiguous distance (UD) under the resulting RSF configuration. With boasted anti-jamming capability, the randomness of carrier frequencies in the RSF configuration implies that the UD is a random variable. In this paper, we aim to depict the UD under the RSF configuration with a deterministic value and find that the theoretical upper bound of random UD, i.e. $\bar{\Lambda}_{rsf}$, play a role. We derive an closed-form expression for the $\bar{\Lambda}_{rsf}$ and further prove that the sufficient and necessary condition for achieving $\bar{\Lambda}_{rsf}$ is the carrier frequencies are relatively prime. With the help of number theory tools, we obtain an elegant expression to approximately describe the probability that the frequencies in the RSF configuration are relatively prime, i.e. P_M . We are inspired to find that, as long as the hop set of the FH waveform

is large enough, P_M approaches 1 when only a dozen of carriers are employed. This conclusion is well supported by numerical simulations and indicates $\bar{\Lambda}_{rsf}$ can serve as a trustworthy metric for the UD under the RSF configuration.

We further study the impact of phase error on the practical UD. Two kinds of phase error, including random noise and multipath induced phase error, are considered. Simulations show that, as long as the number of carriers are increased moderately from a dozen to several dozens, the practical UD can still achieve $\bar{\Lambda}_{rsf}$ with large probability. For a fast frequency hopping waveform, 1000 hops per second for example, the corresponding ranging cycle takes just ten of milliseconds. In contrast, the asymptotical condition for obtaining the theoretical UD under the LSF and PSF configurations are much stricter since one order more carriers and much higher phase SNR are needed respectively.

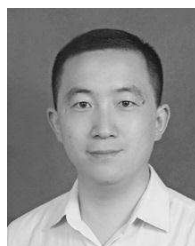
Our work uncovers the feasibility of applying the FH waveform to MCPR systems. Particularly, it reveals that a frequency hopping MCPR system has great potential for large scale radio positioning/navigation applications.

ACKNOWLEDGMENT

The authors would like to thank the anonymous reviewers for their constructive comments and Prof. Xinbing Wang, Dr. Luoyi Fu, and Xinzhe Fu for their valuable feedbacks.

REFERENCES

- [1] J. Kasper and C. Hutchinson, "The omega navigation system—An overview," *IEEE Commun. Soc. Mag.*, vol. 16, no. 3, pp. 23–35, May 1978.
- [2] R. J. Palmer, "Test results of a precise, short range, RF navigational/positional system," in *Proc. IEEE Vehicle Navigat. Inf. Syst. Conf.*, Sep. 1989, pp. 151–155.
- [3] G. Xie, *GPS Principle and Receiver Design*. Beijing, China: Publishing House of Electronic Industry, 2009.
- [4] J. Kreng, M. Sue, S. Do, Y. Krikorian, and S. Raghavan, "Telemetry, tracking, and command link performance using the USB/STDN waveform," in *Proc. IEEE Aerosp. Conf.*, Mar. 2007, pp. 1–15.
- [5] J. B. Berner and S. H. Bryant, "Operations comparison of deep space ranging types: Sequential tone vs. pseudo-noise," in *Proc. IEEE Aerosp. Conf.*, 2002, pp. 1313–1326.
- [6] M. Jankiraman, *Design of Multi-Frequency CW Radars*. West Perth, WA, Australia: SciTech, 2007.
- [7] M. Maróti et al., "Radio interferometric geolocation," in *Proc. ACM Int. Conf. Embedded Netw. Sensor Syst. (SenSys)*, 2005, pp. 1–12.
- [8] X. Li, Y. Zhang, and M. G. Amin, "Multifrequency-based range estimation of RFID tags," in *Proc. IEEE Int. Conf. RFID*, Apr. 2009, pp. 147–154.
- [9] P. J. de Groot, "Extending the unambiguous range of two-color interferometers," *Appl. Opt.*, vol. 33, no. 25, pp. 5948–5953, 1994.
- [10] A. Ranganathan, "Physical-layer techniques for secure proximity verification and localization," Ph.D. dissertation, Dept. Comput. Sci., ETH Zürich, Zürich, Switzerland, 2016.
- [11] L. Wei, W. Qi, P. Liu, E. Yuan, Y. Zhu, and X. Ji, "Method for selecting measurement frequencies based on dual pseudo-random code in radio interferometric positioning system," Chinese Patent 102 221 695, Jun. 12, 2013.
- [12] I. F. Akyildiz, W.-Y. Lee, M. C. Vuran, and S. Mohanty, "NeXt generation/dynamic spectrum access/cognitive radio wireless networks: A survey," *Comput. Netw.*, vol. 50, no. 13, pp. 2127–2159, 2006.
- [13] Y. Zhang, W. Qi, G. Li, and S. Zhang, "Performance of ML range estimator in radio interferometric positioning systems," *IEEE Signal Process. Lett.*, vol. 22, no. 2, pp. 162–166, Feb. 2016.
- [14] I. Vrana, "Optimum statistical estimates in conditions of ambiguity," *IEEE Trans. Inf. Theory*, vol. 39, no. 3, pp. 1023–1030, May 1993.
- [15] T. Rapinoja et al., "A digital frequency synthesizer for cognitive radio spectrum sensing applications," *IEEE Trans. Microw. Theory Techn.*, vol. 58, no. 5, pp. 1339–1348, May 2010.
- [16] D. S. Brian, "The probability that random algebraic integers are relatively r -prime," *J. Number Theory*, vol. 130, no. 1, pp. 164–171, 2010.
- [17] T. M. Apostol, *Introduction to Analytic Number Theory*. New York, NY, USA: Springer-Verlag, 1976.
- [18] F. Yao, *Communication Anti-Jamming Engineering and Practice*, 2nd ed. Beijing, China: Publishing House of Electronic Industry, 2012.
- [19] A. Akhlaq, R. G. McKilliam, and R. Subramanian, "Basis construction for range estimation by phase unwrapping," *IEEE Signal Process. Lett.*, vol. 22, no. 11, pp. 2152–2156, Nov. 2015.
- [20] D. Last, "GNSS: The present imperfect," *Inside GNSS*, pp. 60–64, 2010.
- [21] G. X. Gao, M. Sgammini, M. Q. Lu, and N. Kubo, "Protecting GNSS receivers from jamming and interference," *Proc. IEEE*, vol. 104, no. 6, pp. 1327–1338, Jun. 2016.
- [22] J. K. Ray and M. E. Cannon, "Characterization of GPS carrier phase multipath," in *Proc. ION Nat. Tech. Meeting*, 1999, pp. 243–252.
- [23] P. K. Lee, "Joint frequency hopping and adaptive spectrum exploitation," in *Proc. IEEE Military Commun. Conf. (MILCOM)*, 2001, pp. 566–570.
- [24] R. I. Lackey and D. W. Upmal, "Speakeasy: The military software radio," *IEEE Commun. Mag.*, vol. 33, no. 5, pp. 56–61, May 1995.
- [25] N. Golmie, O. Rebala, and N. Chevrollier, "Bluetooth adaptive frequency hopping and scheduling," in *Proc. IEEE Military Commun. Conf. (MILCOM)*, Oct. 2003, pp. 1138–1142.
- [26] L. Guan, Z. Li, J. Si, and R. Gao, "Generation and characteristics analysis of cognitive-based high-performance wide-gap FH sequences," *IEEE Trans. Veh. Technol.*, vol. 64, no. 11, pp. 5056–5069, Nov. 2015.
- [27] M. K. Simon, J. K. Omura, R. A. Scholtz, and B. K. Levitt, *Spread Spectrum Communications Handbook*, 2nd ed. New York, NY, USA: McGraw-Hill, 2002.



ation and navigation.

PENG LIU received the B. E. and M. E. degrees in computer science and technology from P. L. A. University of Science and Technology, Nanjing, China, in 2004 and 2007, respectively. He is currently pursuing the Ph.D. degree in Communication and Information Systems at P. L. A. University of Science and Technology. He is also a Visiting Scholar at Shanghai Jiao Tong University, China. His research interests include positioning techniques in wireless networks and radio geolocation and navigation.

WANGDONG QI received the Ph.D. degree in communication and information systems from the Institute of Communication Engineering, Nanjing, China, in 1997. He is currently a Professor at P. L. A. University of Science and Technology, Nanjing, China. Some of his research work has been published in the IEEE TRANSACTION ON NETWORKING, SIGNAL PROCESSING LETTERS. He has been an Advanced Visiting Scholar at Polytechnic Institute and State University, Blacksburg, VA, USA. His research interests include wireless networking and security, indoor geolocation, and radio positioning and navigation. He is the PI of some national projects funded by the National Natural Science Foundation of China. Prof. Qi has served as TPC member of IEEE InfoCom from 2011 to 2015.



YUE ZHANG received the Ph.D. degree in computer science and technology from P. L. A. University of Science and Technology, Nanjing, China, in 2014. She is currently an Engineer in the Department of Timing and Frequency, Satellite Navigation Center of Beijing, China. Her research interests include node localization in wireless sensor network and satellite navigation/positioning systems.



LI WEI received the Ph.D. degree in electronic engineering from the Institute of Communication Engineering, Nanjing, China, in 2007. His research interests include signal processing in OFDM systems and Wi-Fi radar and radio localization.

• • •